Jurnal Teknologi, 56 (Sains & Kej.) Keluaran Khas (1), Dis. 2011: 1–25

EROSIVE WEAR OF NATURAL GAS PIPES DUE TO HIGH VELOCITY JET IMPACT: PHYSICAL EXAMINATION AND EXPERIMENTAL STUDY

Z. A. MAJID[1], R. MOHSIN [2] & M. Z. YUSOF[3]

Abstract. A sequential failure of API 5L X42 (NPS8) carbon steel and SDR 17 medium density polyethylene (MDPE) pipes towards the high pressure water pipe was studied. Pipe's failed specimen was physically examined and experimental testing was conducted by using high speed water jetting facility towards a similar NPS8 pipe specimen. High pressure water jet impact from leaked water pipe forms highly erosive water-soil slurry, causing severely damaged on NPS8 carbon steel pipe surface. Thus, it causing substantial losses of pipe coating materials and subsequent rapid thinning of pipe body occurred. Furthermore, weaker ground support causes instability to the MDPE pipe and leads to vertical descend towards high speed gas jet region exerted from failed NPS8 pipe. High impact gas jet physically hit the MDPE pipe at its opposite direction causing its rapid erosion.

Keywords: Liquid impact erosion; gas jet impact; solid particle impact; water jet impact

1.0 INTRODUCTION

Water jet impact can exert enough forces upon a surface resulting to its subsequent physical penetration. Currently, mechanical cutting of materials using blades is being replaced with water cutting, using the principle of water jet. Water jet alone might not be able to contribute major degradation upon any surface, but with the presence of solid particle in the jet stream would result a significant physical damage and might pose bigger threat to the fuel piping system. Failures due to the degradation of piping material could seriously

[1&2] Gas Technology Centre, Universiti Teknologi Malaysia, 81310 UTM Johor Bahru, Johor , Malaysia
[3] School Of Engineering, Universiti Tenaga Nasional 43000 Bangi Selangor, Malaysia
* Corresponding author: zulmajid@fkkksa.utm.my

disrupt supply continuity and posing threat to life and surrounding environment. Cases of natural gas piping failures have proven to be catastrophic as reported by National Transportation Safety Board, USA [1-4].

Erosive wear is a phenomenon of metal degradation due to the repetitive impaction of solid particles entrained in a moving fluid onto any surfaces that directly cause material losses [5]. Slurry erosion which formed by the interaction of solid particles suspended in liquid media with metal surface could easily trigger losses of mass through repeated impacts of particles [6]. This type of erosion has been reported as one of the main source of failure of many engineering equipment such as slurry equipment and hydraulic components [7-11]. This erosive slurry impact may cause serious metal thinning and finally lead to the operational failures of pressurised natural gas pipes [12]. This event could initiate much disastrous incidences especially to those involving escape of flammable gases [1-4].

Early theoretical analyses to predict erosion damage caused by solid particle impact were introduced by Finnie [13, 14] and Bitter [15, 16]. It was later followed by many researchers and majority of their study were focused on erosion wear on a flat surface of various types of materials. It was reported that slurry erosion is an integrating effect of many factors such as particle impact angle [6, 17-22], erodent properties [20, 23-26], and target material [27, 28].

Erosion damage onto curvatured surface such as pipe perimeter surface by erosive slurry materials has not been reported and discussed thoroughly. Study by Lynn *et al.* [29] and Clark *et al.* [30] are two examples for the similar cases. Work of Lynn *et al.* [29] on cylindrical steel specimen described that the erosion rate decreases with the decreasing particle size in suspensions of constant solids loading. It reflects the decrease in the proportion of particles impacting the target surface as well as the decrease in impact velocity. Clark *et al.* [30] has studied the surface profilometry of small cylindrical specimens under impaction of very dilute suspensions of glass beads. The study revealed that the surface profilometry provides the wear depth at each angular location about the specimen whereby no wear is found on the rear face (rearward) of the cylinder. Two noticeable wear mechanisms were identified as deformation and cutting wear acted on ductile material whereas only deformation wear will be applied to erode the brittle material.

A study by Majid *et al.* [12] showed that a leak of high pressure water pipe in a mixture of soil and sand could create erosive slurry impact on nearby pipes

caused its failure. Based on this study, it is proposed that high pressure water impact from leaked water pipe can cause the local wall to thinning the steel pipe body and finally produce a pin hole. However, the mechanism of the erosion was not identified and discussed. Therefore, the aim of this study is to identify, discuss and propose the erosion mechanism of NPS8 and MDPE natural gas pipes due to high velocity jet impact.

2.0 MATERIALS AND METHODS

The study was conducted in two parts; physical examination of failed specimen, and experimental testing. Physical examination involved details study on actual failed pipes sections as received from the incident site. Experimental work was conducted by imposing intense water jetting of 1000 kPa (10 bar) from 5 mm orifice type of leak to a similar pipe specimen. The purpose of the study is to reconstruct the sequence of events experienced by the NPS8 gas pipes under severe water jetting from the opposite water pipe. Results of this experimental study will then be compared to actual data from failed section of the NPS8 steel gas pipe.

3.0 LOCATION AND DESCRIPTION OF THE FAILED PIPES

The failure incident was detected when a pressure drop at the service and city gate station near to the incident location was notified by the Operation and Maintenance Department of a Gas Utility Company. The location of gas pipes leak was evident after the personnel observed a bubbling gas through the watery soil near the road side. The incident caused a 7 hours supply disruption to the customers downstream of the incident locations as shown in Figure 1. Prompt action was taken where the leakages were immediately isolated through valves in order to prevent any release of gas to the surrounding.

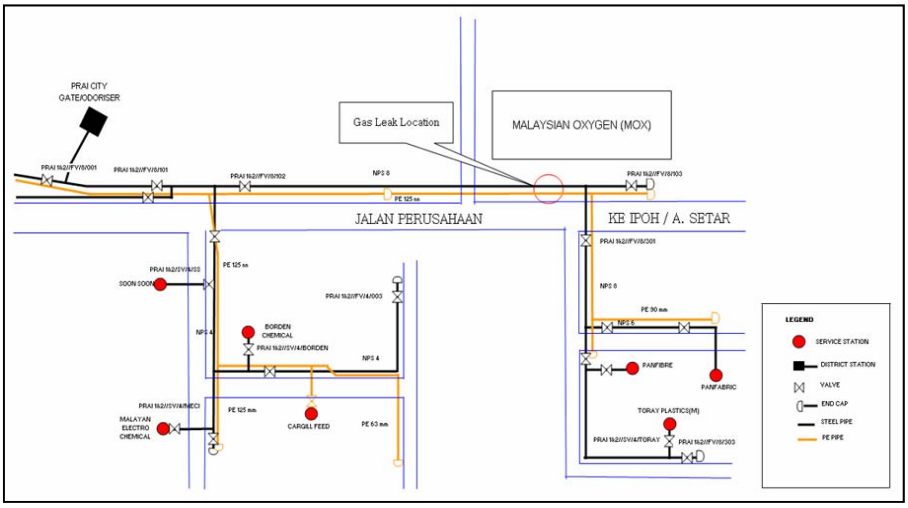

Figure 1 Gas pipes leak location map

Upon excavation at the incident site, there were evident of three pipes; a nominal 8" (203.2 mm) NPS8 carbon steel and MDPE pipes, and a 6" (152.4 mm) asbestos water pipe, with all three indicating signs of serious damages. However, an electrical cable lying parallel to the pipes indicates no apparent sign of physical damage. The NPS8 and MDPE pipes were carrying natural gas at operating pressure of 1800 kPa (18 bar) and 345 kPa (3.45 bar), respectively, prior to shut down. The 6" asbestos pipe was transporting water with an estimated flowing pressure of 1000 kPa (10 bar).

The 8" gas pipe was made of carbon steel, manufactured with stringent specification of NPS8. It was placed around 1.3 m below the ground about 175 mm laterally from the underground water pipe while the water pipe at around 1.2 meter below the surface. The MDPE natural gas pipe is located in parallel with steel and asbestos pipes at a higher position. Comparative positions of the pipes after the excavation and prior (repositioned) to the failure are shown in Figure 2 and 3, respectively.

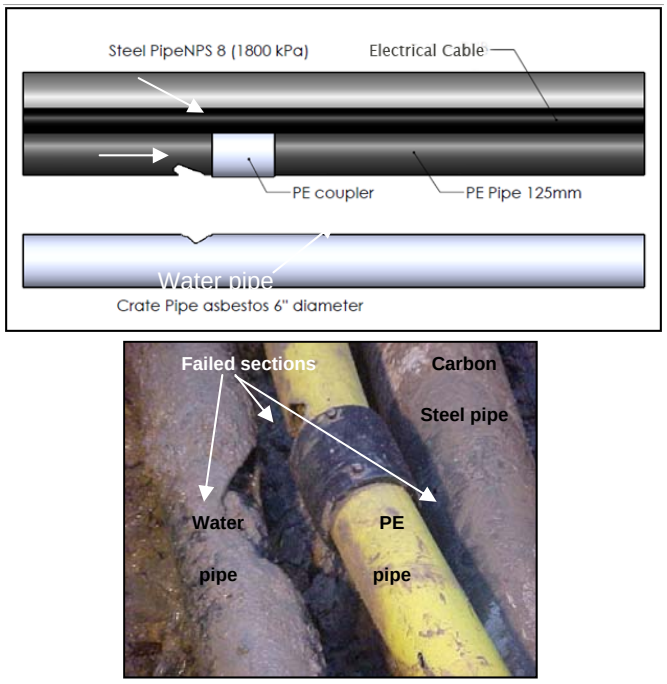

Figure 2 Relative positions of steel NPS8, asbestos and MDPE pipes after the excavation

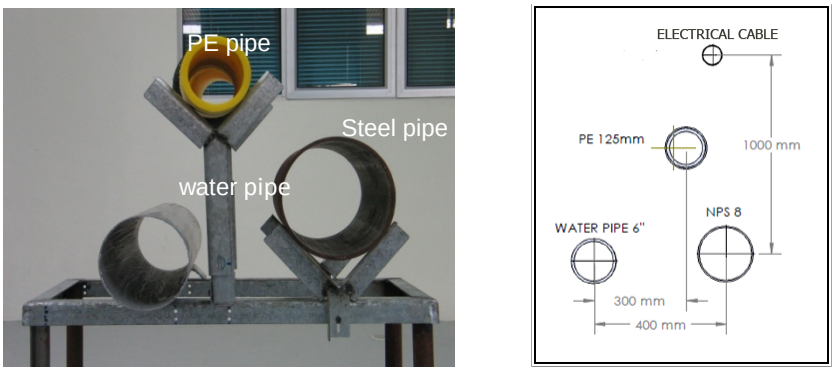

Figure 3 Reconstruction of relative pipe positions in the laboratory

The thicknesses of the NPS8, MDPE and 6" asbestos pipe are 5.6 mm, 11.4 mm and 10 mm, respectively. The NPS8 has been tested hydrostatically at the mill at 15100 kPa (151 bar). Physical parameters of the pipes are shown in

Table 1 and the mechanical and operating data of the pipeline are summarised in Table 2.

Table 1 Physical parameters of pipes

PARAMETERS	NPS8 GAS PIPE	MDPE GAS PIPE	WATER PIPE
Depth cover (m)	1.3	1.2	1.3
Material	Carbon steel	Polyethylene	Asbestos
Internal diameter(mm)	203.2	102.2	152.4
External diameter (mm)	214.4	125.0	172.4
Thickness (mm)	5.6	11.4	10.0
Fluid pressure (Kpa)	1800	345	1000

Table 2 Mechanical and operating data of NPS8 gas pipe

Grade of steel	API 5L X42, 42,000 psi min (yield)
Type of pipe	Seamless
Material	Black carbon
Diameter	214.4 mm
Wall thickness	5.6 mm
Hydraulic pressure (factory tested)	15100 kPa (151 bar)

Table 3 shows the chemical composition of the NPS8 carbon steel pipe. Combustion and infrared detection method according to ASTM E1019 was employed to analyse the carbon and suplhur content. The remaining elements were evaluated through X-ray fluorescence (XRF) following the standard outlined in ASTM E1085.

Table 3 Chemical composition (wt %) of NPS8 gas pipe

COMPONENT	WT %	COMPONENT	WT %
C	0.18	Ni	0.02
Si	0.22	Mo	0.01
Mn	0.84	Ti	0.001
P	0.013	Co	0.06
S	0.004	B	0.0001
Cu	0.03	Ca	0.00023
Cr	0.07	Al	0.03

4.0 PHYSICAL EXAMINATION ON FAILED SPECIMENS

4.1 Visual Inspection

Visual inspections were carried out on both, the photographic evidence and two pipes as shown in Figures 4 and 5. The exposed part of the steel pipe (with the coatings eroded) was heavily oxidized (Figures 4b and 5a). The original condition of the exposed part (Figure 6b) was found free from coating material with clean smooth and shining condition after the incident. Howeverthe presence of an erosion marks on the pipe surface in a ripple liked shape (Figure 7a) is similar to the report by Hasan *et al.* [31]. No exhibit of scale or deposit was observed on the inside surface of the pipe thus dismay any indication of internal corrosion.

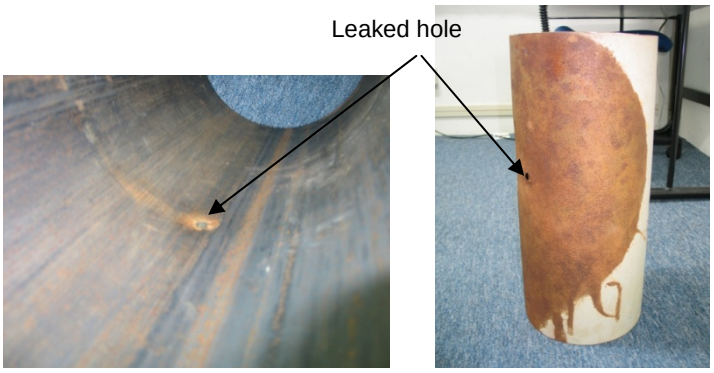

a. Internal condition b. External surface condition

Figure 4 Failed specimen of NPS8 gas pipe

Figure 5 Damaged MDPE gas pipe showing serious shear remnants of sand blasting impact

a. Oxidized NPS8 carbon steel pipe indicating leak section

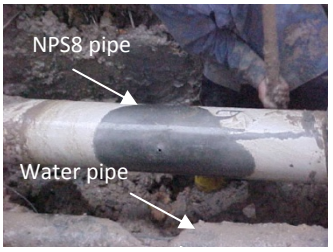

b. NPS8 carbon steel pipe at incident site

Figure 6 Surface condition of failed NPS8 carbon steel pipe

a. Overall view of hole b. Closed up view

Figure 7 A 10 mm diameter hole on NPS8 gas pipe wall

A hole with an average diameter of 10 mm was evident in the middle of the eroded part of the carbon steel pipe section (Figure 7a). The eroded part was found to be smooth and free from rust. The size of the eroded section was measured around 50 cm by 30 cm (Figure 7b). The absence of scratch marks or dents in the vicinity of the eroded part seems to support the statement that no third party work was involved within the vicinity of incident location.

4.2 SURFACE PROFILOMETRY

Surface profilometry was conducted using two specimens (A and B) which were obtained from two locations around failure section at about 50 mm apart, schematically shown in Figure 8. Results obtained indicated that the thickness of the metal decreased substantially against the identified leak point as illustrated in Figure 9a for specimen A and Figure 9b for specimen B. Continuous metal losses surrounding the impact area of water jetting had initiating a serious crack growth (pinhole) caused by drastic erosion process. Figure 10 indicates jetting direction and its dispersion against NPS8 pipe wall that had caused erosive wear on pipe wall.

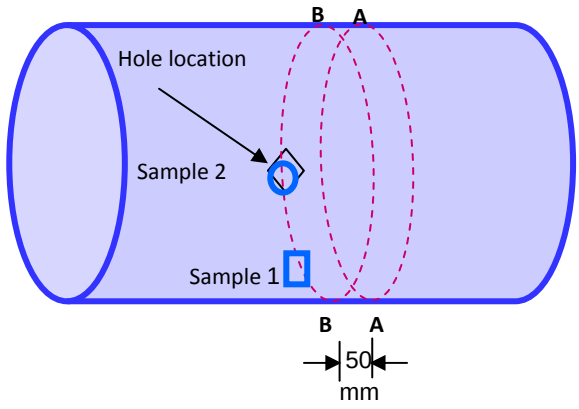

Figure 8 Thickness mapping areas and specimen locations of NPS8 gas pipe

A

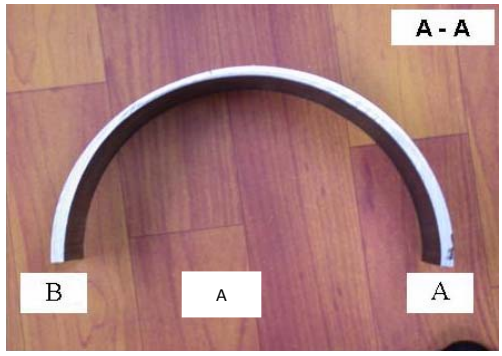

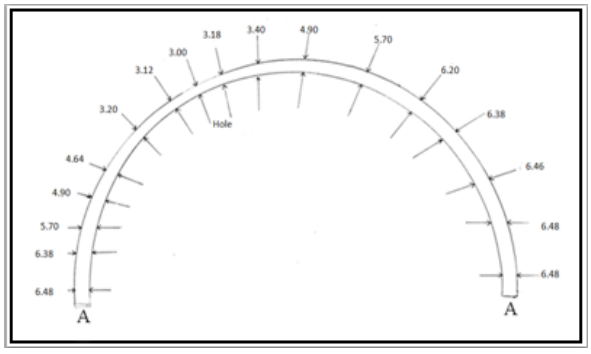

a. Thickness mapping for section A - A (50 mm away from hole)

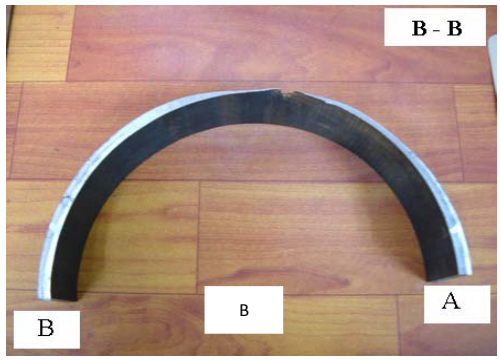

B

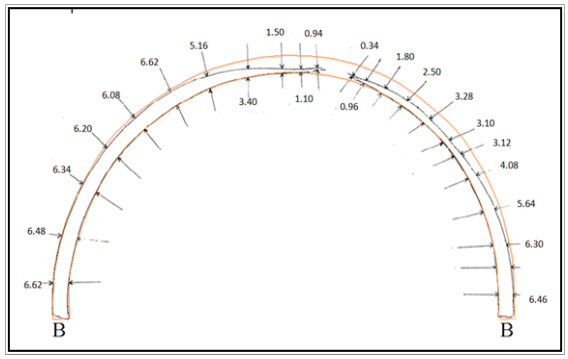

b. Thickness mapping for section B - B (half way through the hole)

Figure 9 Thickness mapping of NPS8 gas pipe

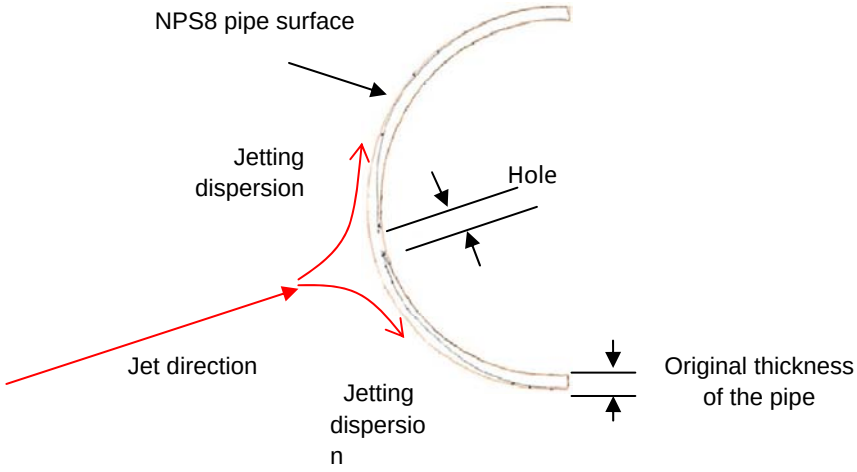

Figure 10 Jet dispersion around pipe wall

Assessment of this results revealed that the thickness of the pipe decreased substantially only at area against to the jetting orifice position. Pipe metal loss has occurred on the area facing directly to the water pipe orifice jet resulting in a hole which increased in its dimensional size with severed metal losses (Figures 2 and 6b). This indicates that the hole was caused by drastic erosion from the failed water pipe buried in the vicinity of the gas pipe. This phenomenon is further explained in Figure 11. By considering the estimated jetting of 20°, it is found that the jetting direction is directly hit the area that had severly experiencing the thickness reduction. The surface pattern was similar with the finding made by H. McI. Clark [12] on cylindrical specimen using slurry pot erosion tester as shown in Figure 12 [32]. There are two peculiar areas that had experienced two different types of wear mechanism. The centre part which is directly hit by the water jetting at high angle where the water is the dominant erosive medium will erode according the deformation wear mechanism. The surrounding areas in the other will erode following cutting wear mechanism. These two types of wear mechanism was proposed by Finnie [13-14], Bitter [15-16], and Neilson *et al.* [33].

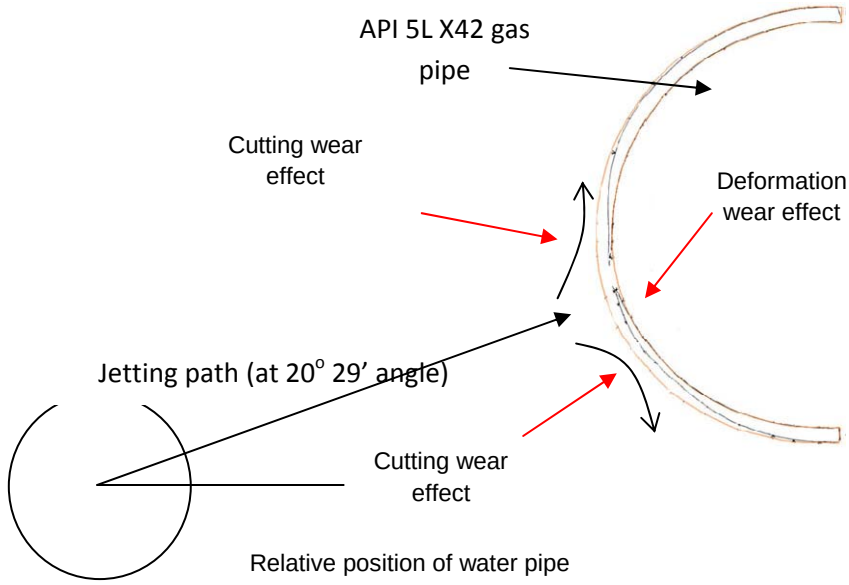

Figure 11 Rearrangement of pipe surface shows rapid thinning of pipe surface facing toward water jetting

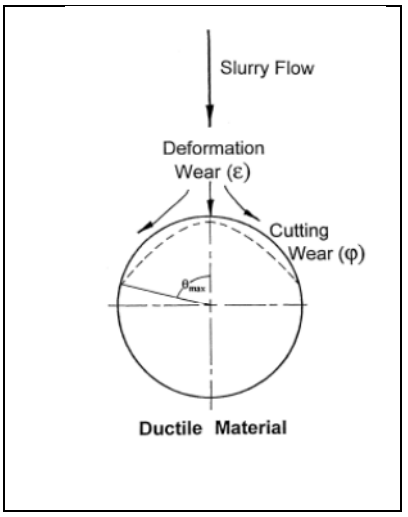

Figure 12 Schematic diagram of slurry flow and distribution of deformation wear and cutting wear on a ductile material

Rapid thickness reduction is also clearly illustrated in Figure 13. Thickness reduction show significant reduction toward the leaked hole. The reduction pattern found to be similar with the wear depth reported by Clark *et al.* [34-35]. As the pipe behaved as a ductile material, it will be eroded through cutting wear mechanism. The estimated jetting angle of 20° which is at low angle just suitable to performed that type of mechanism. This finding is in agreement with study reported by Neilson *et al.* [33].

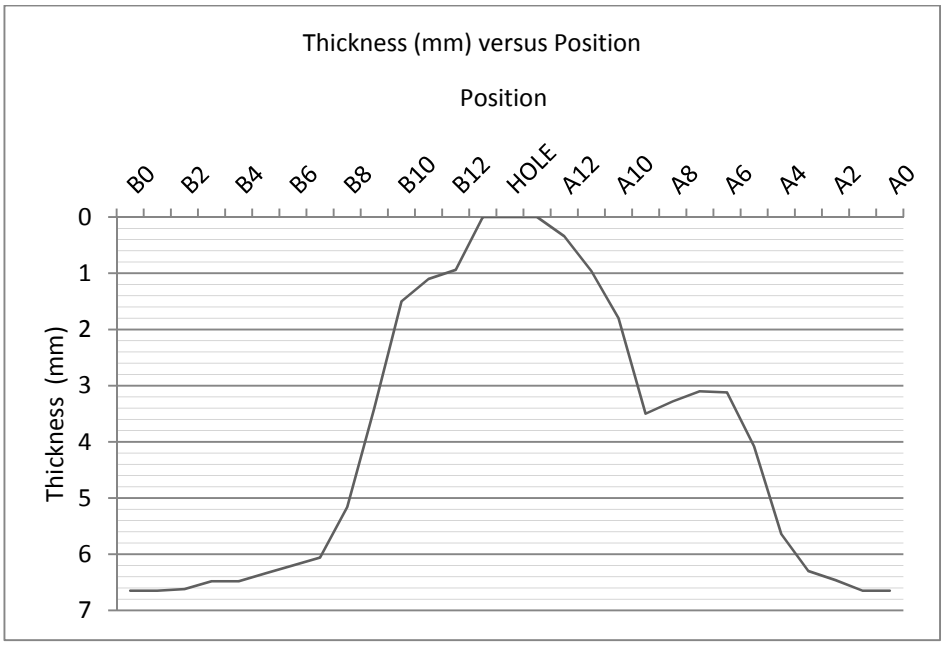

Figure 13 A Plot of thickness reduction

5.0 EROSION CHRONOLOGY

Initial assessment suggests that the asbestos water pipe operating around 1000 kPa (10 bar) with 10 mm wall thickness was the first to fail. The leak could have caused high pressure water jetting which, in the presence of surrounding soil and sand materials, could have produced highly erosive slurry. This erosive slurry was produced as the water jet swept the suspended sand and silt along its direction prior to the impact onto the pipe surface. This slurry could have continuously hitting on the NPS8 steel pipe, causing the erosion of the coating materials and thinning the pipe wall.

High pressure water jetting from leaked water pipe had earlier caused the substantial displacement of the supporting soil materials underneath the MDPE, shifting downwards. When the steel gas pipe leaked, MDPE pipe was pushed further down until it was low enough to be '*in the line of fire*' from the high pressure gas jet (Figures 14 and 15).

Visual inspection of the photographic evidence of the incident and the damaged pipe specimens had led to initial conclusion that the most probable cause of MDPE pipe failure was due to high pressure gas jet from NPS8 steel leakage. The continuous gas jet swept the water and suspended sand and silt onto the surface of MDPE pipe causing a *'wet sand blasting'* phenomenon. Similar case was also reported by Hasan *et al.* [31]. This is most evident from the final location of the MDPE pipe relative to the NPS8 pipe leak and the erosion pattern found on the MDPE pipe damaged area shown by Figures 5, 14 and 15. The sharp and ragged surface condition is an evident of high pressure sandblasting effect of gas jet from the leaked NPS8 pipe onto MDPE pipe wall.

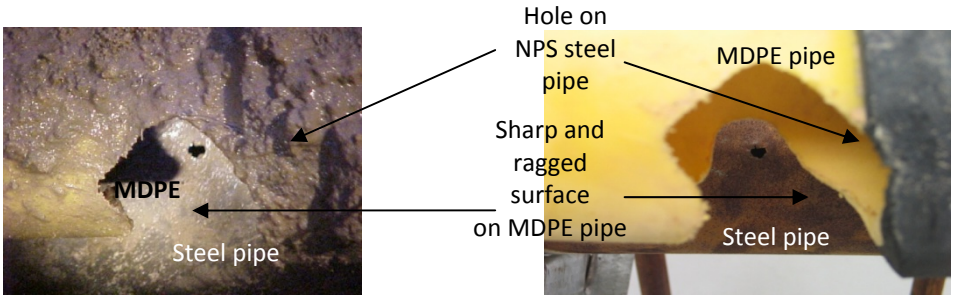

Figure 14 In-situ MDPE pipe relative position directly *'in the line of fire'* NPS8 gas jet

Figure 15 Repositioning of NPS8 and MDPE pipe in laboratory (after the excavation)

6.0 EXPERIMENTAL STUDY

This experimental study is aimed to identify the erosion pattern on NPS8 steel pipe. Results obtained from this experimental work will be compared to actual physical observations from failed section of the steel gas pipe specimen.

6.1 Experimental Setup

Experiment was conducted by utilising a static compartment (experimental tank) to simulate surrounding environment of an underground piping system. A short section of a piping system was placed in the compartment to stimulate the actual working natural gas piping. A river sand acts as backfilling material which filled into the compartment. This sand will represent the erosive particles suspended in the water jet stream. Water jetting effect was created in the compartment by using different sizes of orifice pointing towards the buried pipe.

A section of natural gas pipe used in this particular experiment was attached to a saddle on the rig. The saddle was adjusted vertically to an appropriate distance suitable for the experiment. An orifice was attached to the orifice holder. Supply pressure of the water was set at 1000 kPa (10 bar) while the distance away from the jetting source was varied from 10-70 cm. Typical river sands has been employed as backfilling materials, a similar practice for a construction of gas pipeline trenching system. It has been sieved to a size ranging from 600-2000 μm to resemble the typical size for backfilling sand used to support the pipe. These erodents were filled into the handling tank prior to lowering-in piping rig into the tank.

A number of small holes have been drilled at specific locations on the rig structure that will provide repelling force created by 'small jet-push effect' to further disperse surrounding sand particles in the tank, allowing the rig to be lowered down into the sand thus burying it. After designated time interval, the rig was lifted-out from the handling tank using a chain block lifting system. The thinning rate of the sample pipe material was measured on points dictated based on a data-taking template as depicted in Figure 16. Figure 17 is a schematic diagram that represents experimental rig used in this particular study.

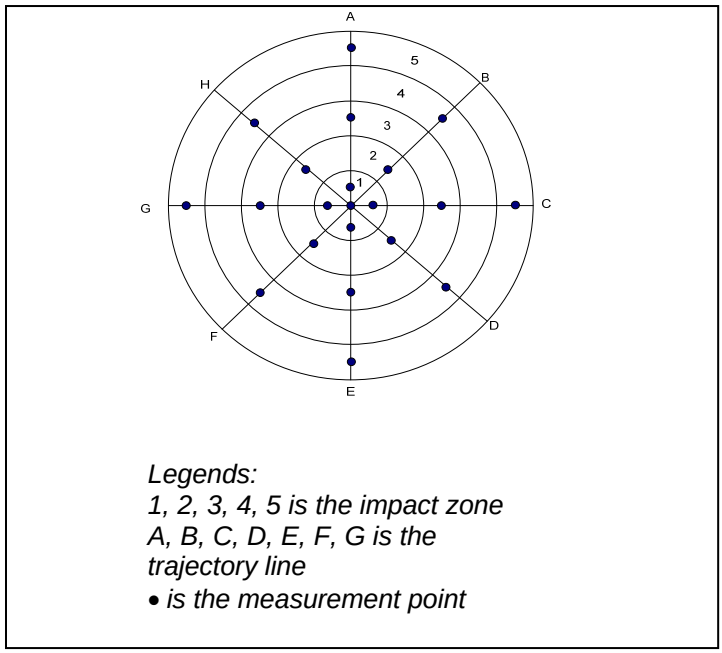

Figure 16 Data taking template

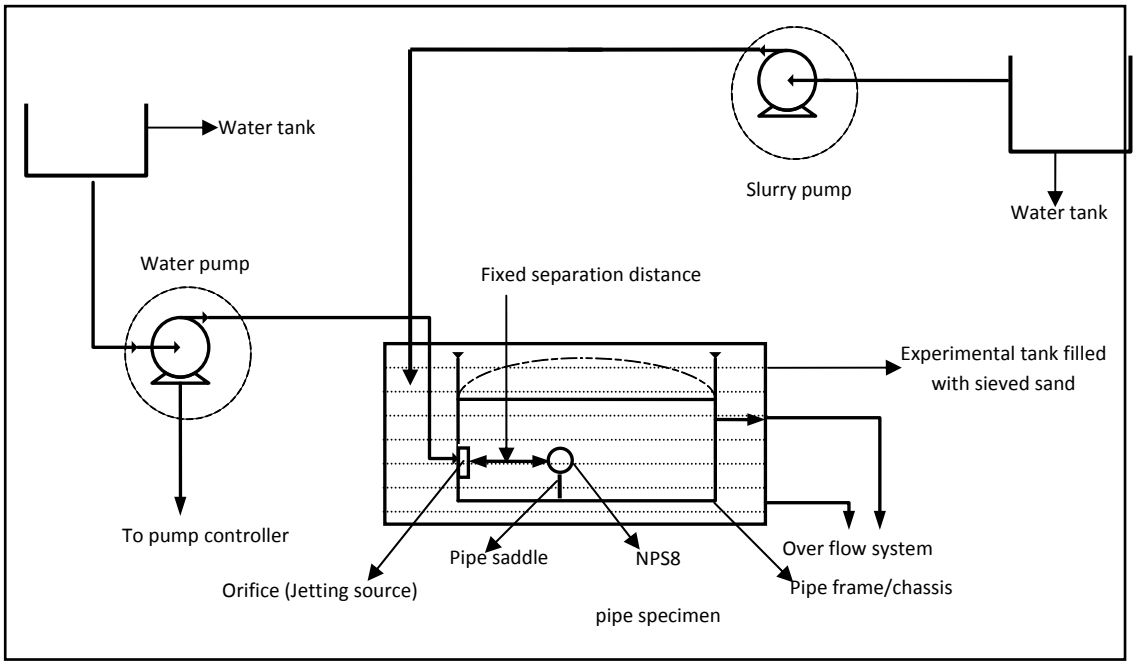

Figure 17 Experimental set up

6.2 Experimental Results

6.2.1 Physical Examination Of Impacted Surface

Physical examination of the impacted surface showed that orifice jetting produced significant marking impact on the pipe specimen resembling a rounded shape. One thing peculiar about the impacted surface is that the roughness of the impacted surface is not evenly scattered. This is indicated by the existence of two distinct areas on the specimen's surface, with one being smooth while the other being very rough having rippled like marks. These marks show great similarity with the marks found on the failed pipe section (Figure 7a). Similar marks were found by Hasan *et al.* [31] in his work of consequential rupture of gas pipeline. Figure 18 below depicted a specimen surface after an exposure of 48, 72 and 100 hours respectively to erosive jet impact.

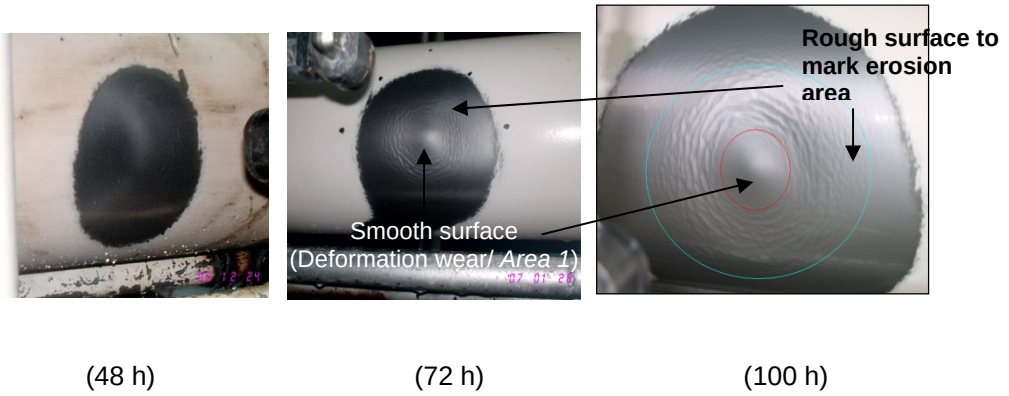

Figure 18 Specimen surface after impact

Two distinct impact patterns could be seen clearly on the impact surface. Impact pattern upon these two areas could be characterized by mode of impact medium either water or sand as the major contributor in the erosion media. *Area 1* has a smoother surface compared to the *Area 2* and this can be explained by Figure 19.

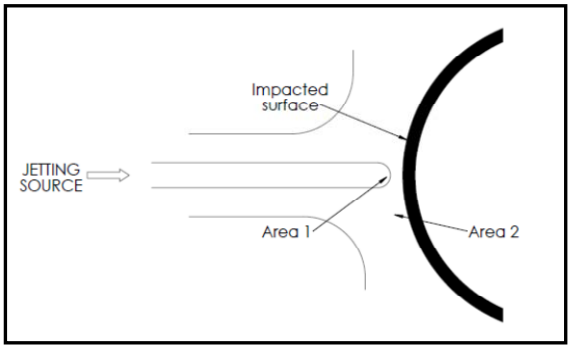

Figure 19 Orifice jetting profiling

Due to water velocity differences between *Area 1* and *Area 2*, different erosion rate had been experienced by these two areas. It may had resulted to the differences of sand carrying ability (ability of the jet stream to induce and carrying the erosive media (sand particles)) of the water jet stream. In this particular case, various velocities of several impact areas in the water jet stream had resulting differences in the erosion rate. As such, velocity of the orifice outlet in *Area 1* was found higher compared to its subsequent *Area 2* (deformation wear) [32]. Therefore its ability to carry sand particles is subsequently reduced. The acting weight of sand particles reduce the ability of sand particles' to move with higher velocity in Area 1, thus causing a cutting wear. Similar finding had been reported by H. McI. Clark [32]. The erosion mechanism for ductile material suggested by Finnie [13, 14], Bitter [15, 16], and Neilson *et al.* [33] which postulated that the 'erosion by cutting' will act upon low angle direction whilst 'erosion by deformation' implied for high angle direction, both applied in these two peculiar areas.

Evidence of sand particles mixing with the water jet stream can be seen through the identification of the rough surface (ripple like) on the impact area. Characteristics of the jet reflected by round-shape on the specimen's surface were due to its relative rounded jet outer orifice. Thus, it is concluded that the smooth surface in the middle stream impact area is represented by a smooth rounded area being a result of a horizontal tunneling. The impacted surface confirmed the hypothetic statement of zero sand particles at the point of impact. An impression of a hollow like structure formation from the orifice outlet which resembles a tunnel could be seen clearly in Figure 18. This is

exactly the weakest point of the pipe that initially started a pinch which later becomes evident shown in Figures 4, 6 and 7. This also agreed upon the final ruptured specimen from the experiment shown in Figure 20.

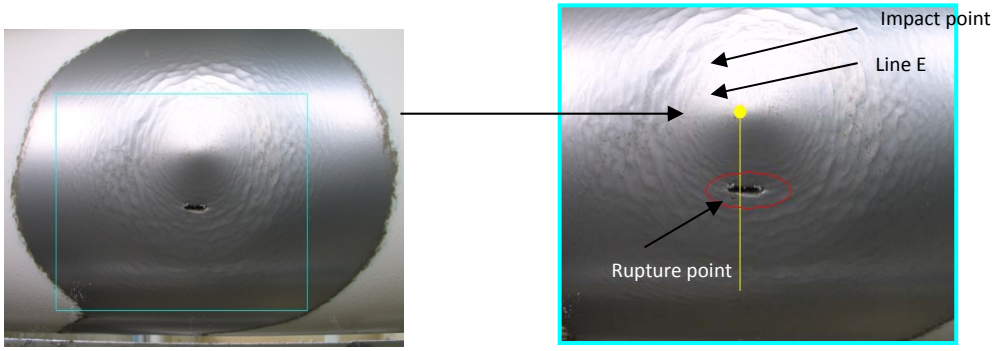

a. Overall picture of ruptured specimen b. Close-up of the rupture point

Figure 20 Picture of ruptured specimen from the experiment

6.2.2 Specimen Thickness

The relationship between pipe thickness and time is inversely proportional, decreasing with the increment of time (Figures 21-23). During experiment, pipe specimen was experiencing continuous erosion due to erosive water jetting. The rate of thinning in *Zone 1* (target template – Figure 16) is higher compared to other zone regardless of its streamlines and locations. This could be further explained by the fact that during the jetting operation, tunneling effect was evident. Thus, *Zone 1* eroded at a higher rate compared to the rest of the zone. This phenomenon is largely contributed by the effect of concentrated impact of erosive sand slurry hampering to *Zone 1* area which coincides with *Area 2* of the tunneling section.

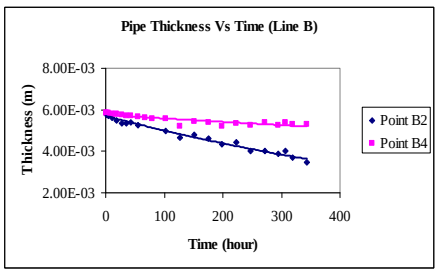

Figure 21 Thickness graph for line A

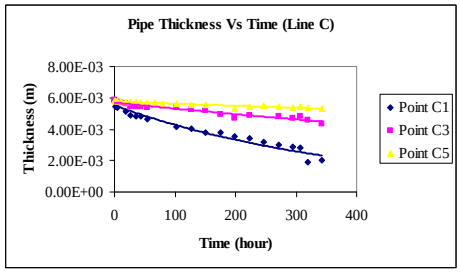

Figure 22 Thickness graph for line C

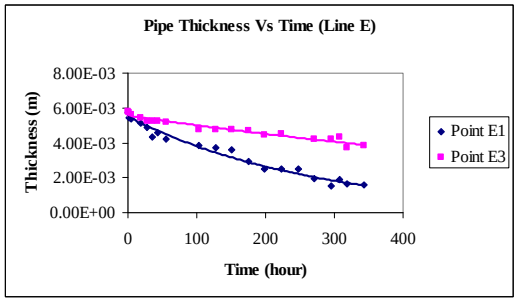

Figure 23 Thickness graph for line E

The average thinning rate of each point was obtained by dividing the thickness loss to the total period of experiment. Table 4 denotes each point's average thinning rate of the specified point due to water jetting. Points indicated in the Table 4 were based on the marking points rendered by the designated template design shown in Figure 16. Data shown in Table 4 indicates that the highest thinning rate is running across line E while the lowest thinning rate is evident in the line A. This could be explained by the existence of vertical tunneling near Line A and turbulent flow area near line E as shown in Figure 24.

Table 4 Average thinning rate

Point	Average Thinning Rate (m/hr)
A1	1.08×10^{-5}
A3	2.87×10^{-6}
A5	1.01×10^{-6}
B2	6.84×10^{-6}
B4	1.60×10^{-6}
C1	1.10×10^{-6}
C3	4.46×10^{-6}
C5	1.41×10^{-5}
D2	1.23×10^{-5}
D4	3.28×10^{-6}
E1	1.21×10^{-5}
E3	5.73×10^{-6}

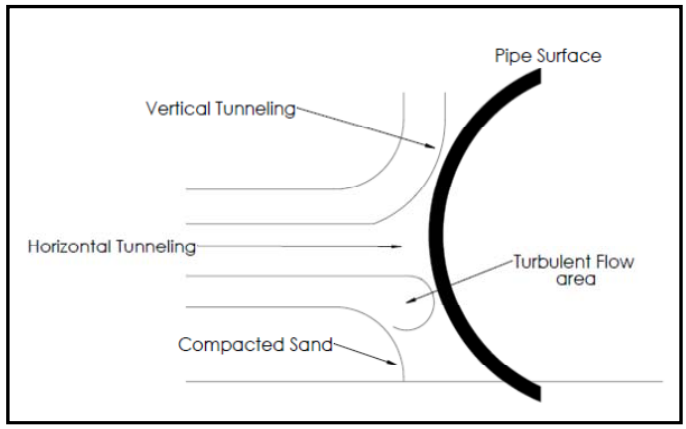

Figure 24 Tunnel profiling

7.0 CONCLUSIONS

This study was intended to identify, discuss and propose the mechanism of the erosion of NPS8 carbon steel and MDPE natural gas pipes due to high velocity jet. Visual examination and experimental works were performed and the following conclusions can be drawn:

(1) The deformation and cutting wear mechanism was found to be the mechanism of erosion that caused the thinning NPS8 carbon steel pipe-wall. This is when the thinning process reached a certain level of minimum wall thickness the inside gas-pressure of 1800 Kpa start to develop a pin hole damage that pointing outwards.
(2) The MDPE pipe was failed by the impaction of intense pressure gas jet from NPS 8 carbon steel pipe.
(3) The erosion sequence can be summarised as follows:
    (a) The water jet from leaked water pipe mixed with soil and silt to form water slurry with high erosive properties which its impact upon the pipe surface causing the loss of pipe coating materials. Continuous impaction of these erosive slurries subsequently led to the rapid thinning of the NPS8 carbon steel pipe body before its failure.
    (b) High pressure jet from leaked water pipe that had earlier caused significant displacement of the supporting soil materials underneath the MDPE pipe causing it to move further downwards to a maximum displacement of around 200 mm, where it was impacted by the high velocity and intense pressure gas jet from NPS8 carbon steel pipe.

ACKNOWLEDGEMENT

Authors are most grateful and wish to all members of Gas Technology Center (GASTEG) Pipeline Failure Team for their significant efforts and commitments in conducting experiments and simulation throughout research period. Gas Malaysia Sdn. Bhd. (GMSB) is also highly acknowledged for providing pipe samples and continual financial support.

REFERENCES

[1] National Transportation Safety Board. 1996. Pipeline Accident Report: Natural Gas Pipeline Rupture and Fire During Dredging of Tiger Pass, Louisiana, National Transportation Safety Board, Washington. 1-50.

[2] National Transportation Safety Board. 1998. Pipeline Accident Report: Natural Gas Pipeline Rupture and Subsequent Explosion St Cloud, Minnesota, National Transportation Safety Board, Washington. 1-45.

[3] National Transportation Safety Board. 2001. Pipeline Incident Report, Natural Gas Pipeline Rupture and Fire in South Riding, National Transportation Safety Board, Washington. 1-20.

[4] National Transportation Safety Board. 2003. Pipeline Incident Report, Natural Gas Pipeline Rupture and Fire, Near Carlsbad, New Mexico, National Transportation Safety Board, Washington. 1-12.

[5] I. M. Hutchings. 1974. Particle Erosion of Ductile Metals: A Mechanism of Material Removal. *Wear*. 27: 121-128.

[6] M. A. AI-Bukhaiti, S. M. Ahmed, F. M. F. Badran, K. M. Emara, 2007. Effect of Impingement Angle on Slurry Erosion Behaviour and Mechanism of 1017 Steel and High-chromium White Cast Iron. *Wear*. 262: 1187-1198.

[7] R. Hamzah, D. J. 2004. Stephenson, J. E. Strutt. Erosion of Materials used in Petroleum Production. *Wear*. 186: 493-496.

[8] R. J. Llewellyn, S. K. Tick, K. F. 2004. Dolman, Scouring Erosion Resistance of Metallic Materials used in Slurry Pump Service. *Wear*. 256: 592-599.

[9] F. Aimin, L. Jinming, T. Ziyun, 1995. Failure Analysis of the Impeller of Slurry Pump Subjected to Corrosive Wear. *Wear*. 181-182: 876-882.

[10] K. Haugen. O. Kvernvold, A. Ronold, R. Sandberg, 1995. Sand Erosive of Wear-resistance Materials: Erosion in Choke. *Wear*. 186-187: 179-188.

[11] M. A. Al Bukhaiti, F. M. F. Badran, K. M. Emara, S. M. Ahmed. 2002. Slurry Erosion Parameters-a review. In: The 3rd Assiut University Int. Conf. on Mech. Eng. Advanced Tech. for Ind. Application, Assiut, Egypt, December.

[12] Z. A. Majid, R. Mohsin, Z. Yaacob, Z. Hassan. 2010. Failure Analysis of Natural Gas Pipes, Engineering Failure Analysis. 17: 818-837.

[13] I. Finnie, 1960. Erosion of Surfaces by Solid Particles. *Wear*. 3: 87-103.

[14] I. Finnie, 1972. Some Observation on the Erosion of Ductile Metals. *Wear*. 19: 81-90.

[15] J. G. A. Bitter, 1962. A Study of Erosion Phenomena Part I. *Wear*. 6: 5-21.

[16] J. G. A. Bitter, 1962. A Study of Erosion Phenomena Part II. *Wear*. 6: 169-190.

[17] K. Suguyama, K. Harada, S. Hattori, 2008. Influence of Impact Angle of Solid Particle on Erosion by Slurry Jet. *Wear*. 2657: 13-120.

[18] G. R. Desale, B. K. Gandhi, S. C. 2008. Chain, Slurry Erosion of Ductile Materials under Normal Impact Condition. *Wear*. 264: 322-330.

[19] G. T. Burstein, K. Sasaki, 2000. Effect of Impact Angle on the Slurry Erosion-corrosion of 304L Stainless Steel. *Wear*. 14080-94.

[20] H. McI. Clark, K. K Wong, 1995. Impact Angle, Particle Energy and Mass Loss in Erosion by Dilute Slurries. *Wear*. 186-187: 454-464.

[21] F. Lin, H. Shao, 1997. The Effect of Impingement Angle on Slurry Erosion. *Wear*. 141(1991): 279-289.

[22] T. I. Oka, H. Ohnogi, T. Hosokawa, M. Matsumura, The Impact Angle Dependence of Erosion Damage Caused by Solid Particle Impact. *Wear*. 203-204: 573-579.

[23] G. R. Desale, B. K. Gandhi, S. C. Chain, 2006. Effect of Erodent Properties on Erosion Wear of Ductile Type Materials. *Wear*. 261: 914-921.

[24] H. McI. Clark, 2002. Particle Velocity and Size Effects in Laboratory Slurry Erosion Measurement OR do you know what your Particles are Doing? *Tribology International*. 35: 617-624.

[25] H. McI. Clark, R.B. Hartwich, 2001. A Re-examination of the 'Particle Size Effect' in Slurry Erosion. *Wear*. 2481: 47-161.

[26] Z. Feng, A. Ball, 1999. The Erosion of Four Materials using Seven Erodents-towards an Understanding. *Wear*. 233-235: 674-684.

[27] M. Divakar, V. K. Agarwal, S. N. Singh, 1995. Effect of the Material Surface Hardness on the Erosion of AISI316. *Wear*. 259: 110-117.

[28] N. P. Abbade, S. J. Crankovic. 2000. Sand-water Slurry Erosion of API 5L X65 Pipe Steel as Quenched from Intercritical Temperature.*Tribology International*. 33: 811-816.

[29] R. S. Lynn, K. K. Wong, H. McI. Clark, 1991. On the Particle Size Effect in Slurry Erosion. *Wear*. 149: 55-71.

[30] H. McI. Clark, R. B. Hartwich, 2001. A Re-examination of the 'Particle Size Effect' in Slurry Erosion. *Wear*. 248: 147-161.

[31] F. Hasan, J. Iqbal, Consequential Rupture of Gas Pipeline, 2006. *Engineering Failure Analysis*. 13: 127-135.

[32] H. McI. Clark, 1993. Specimen Diameter, Impact Velocity, Erosion Rate and Particle Density in a Slurry Pot Erosion Tester. *Wear*. 162-164: 669-678.

[33] J. H. Neilson, A. Gilchrist, 1968. Erosion by a Stream of Solid Particles. *Wear*. 11: 111-122.

[34] H. McI. Clark, K. K. Wong, 1995. Impact Angle, Particle Energy and Mass Loss in Erosion by Dilute Slurries. *Wear*. 186-187: 454-464.

[35] H. McI. Clark, R. B. Hartwich, 2001. A Re-examination of the 'Particle Size Effect' in Slurry Erosion. *Wear*. 248: 147-161.